Cylindrical Micelles in Rigid–Flexible Diblock Copolymers

ARTICLE *in* MACROMOLECULES · JUNE 1992

Impact Factor: 5.8 · DOI: 10.1021/ma00039a040

2 AUTHORS, INCLUDING:

Glenn H Fredrickson
University of California, Santa Barbara

434 PUBLICATIONS **28,369** CITATIONS

Reprinted from Macromolecules, 1992, 25.

Cylindrical Micelles in Rigid–Flexible Diblock Copolymers

D. R. M. Williams* and G. H. Fredrickson

Departments of Materials and Chemical & Nuclear Engineering, University of California, Santa Barbara, California 93106

Received June 13, 1991; Revised Manuscript Received October 8, 1991

ABSTRACT: We present a theoretical study of a melt of diblock copolymers consisting of a rigid rod and a flexible tail. It is shown that, in addition to the lamellar phases previously discussed, there also exist phases of "hockey puck" micelles, where the rods are packed axially into cylinders. These phases occupy most of the phase diagram previously thought to consist of monolayer lamellae. It is argued that spherical micelles probably do not exist.

1. Introduction

In a recent paper[1] (hereafter referred to as [SV]), Semenov and Vasilenko initiated a study of melts of diblock copolymers consisting of a flexible tail connected to a rigid rod. They assumed that the tail and rod segments were incompatible, with the degree of incompatibility described via a Flory parameter χ_S. In general, one expects χ_S to be large at room temperature because of the large chemical differences between stiff rods and flexible chains. At low enough χ_S values the system exhibits a nematic phase (provided the rod volume fraction is sufficiently large) which, as the interaction parameter is increased, changes to a smectic phase. As χ_S is further increased the smectic phase was predicted to undergo various other changes—first to a complete monolayer regime where the chains are expelled completely from the rigid rod monolayers and then to a bilayer lamellar phase. If the volume occupied by the flexible tails is small, then the phases studied in [SV] are probably the most stable. In this paper we study the possibility of forming discrete micellar phases. One expects these to be stable in the limit where the flexible tail volume fraction is large.

At any given temperature the phase which is most stable is mainly determined by a balance between the Flory term, which favors separation of the rods and chains, and a chain stretching term. Because in a block copolymer the chains are permanently attached to the rods, complete separation is never possible and there is always some interface between the two. In general, the sharper the interface, the more the chains have to stretch and the larger is the stretching free energy. At large values of χ_S the system can be modeled as a set of chains grafted to a wall, forming a polymer brush. Once this limit has been achieved the geometry of the brush becomes important. Infinitely wide flat brushes (i.e., lamellae) pay a large stretching penalty. This penalty is governed by how rapidly the volume away from the surface increases with distance r. For an infinite planar brush it increases only as r, whereas for an infinitely long cylinder and a sphere it goes as r^2 and r^3, respectively. As chains are less confined and hence less stretched in the latter cases, one might expect cylindrical and spherical micelles to exist in some regions of the phase diagram. For ordinary diblocks consisting of two flexible blocks this is in fact the case.[2-5] However, for rod–coil diblocks there are extreme steric problems associated with packing the rods radially into a cylinder or a sphere. For this reason we propose the existence of cylindrical disklike micelles. These are micelles consisting of pieces of lamellae cut into cylinders. Their main advantage relative to lamellae consists of enabling the chains grafted onto their top and bottom surfaces to fan out into a larger region of space (ultimately increasing as r^3) and hence stretching less. Their main disadvantage is the creation of an extra "curved" surface, for which they pay a surface energy penalty. It is the balance between these two terms that decides whether they are more favored than lamellae. In this paper we shall use the terms puck and cylinder interchangeably, although "puck" reflects the rather flat character of the micelles more accurately.

Similarly shaped micelles have been predicted theoretically, using scaling approaches, in rod–coil diblocks in a selective solvent[6] and in coil–crystalline diblocks, again in a selective solvent.[7] There has also been one numerical study of coil–crystalline diblocks in a melt,[8] although only the lamellar case was addressed. There also exist many studies of polymers consisting of alternating liquid crystalline and flexible monomers.[9-13] It has been predicted that[12] such systems form "sheafs" under appropriate conditions, for which the core resembles the cylindrical micelle cores described here.

We begin by summarizing the phases found by Semenov and Vasilenko,[1] in section 2. In section 3 we derive an expression for the chain-stretching free energy for a cylindrical micelle. This is in practice the most difficult part of the calculation because of the lack of symmetry in the problem. In section 4 the free energy of the two possible hockey puck phases is calculated and compared to the two types of complete lamellar phases found in [SV] and also to the incomplete monolayer regime. This allows us to draw an amended phase diagram for the system, which includes two hockey puck phases. In section 5 we briefly discuss the possibility of radially packed cylindrical and spherical micelles. Section 6 contains a discussion of the phase diagram.

2. Nematic and Smectic Phases

We begin with some definitions. We set Boltzmann's constant equal to unity throughout and express all free energies in units of k_BT. We consider rods of length L and cross-sectional area d^2 where $d \ll L$. The flexible part of the blocks is assumed to consist of N segments of volume v with a mean-square separation between adjacent segments of $6a^2$ in the unperturbed melt state. We use the same dimensionless parameters as [SV], namely

$$\lambda = \frac{Nv}{Ld^2} = \frac{\phi}{1-\phi} \tag{1}$$

$$\kappa = Na^2/L^2 \tag{2}$$

and

$$\nu = \kappa/\lambda \tag{3}$$

Here ϕ is the volume fraction occupied by the chains. In

0024-9297/92/2225-3561$03.00/0

[SV] it is shown that ν is proportional to the ratio of the chain persistence length to the rod length, and hence $\nu \ll 1$. Here, unlike in [SV], we leave all lengths dimensional.

One point concerning the calculation in [SV] first needs to be made. If $\eta(\mathbf{r})$ and $g(\mathbf{r})$ are the local volume fractions of rods and coils, respectively, then the expression used in [SV] for the Flory interaction energy term is (in dimensional units)

$$F_{at} = \frac{\chi_S}{Ld^2}\int d^3\mathbf{r}\, \eta(\mathbf{r})\, g(\mathbf{r}) \tag{4}$$

This has the unfortunate property that if the length of the rods is doubled while keeping the volume fraction of the rods constant, the free energy is halved (unless χ_S is doubled). This is a rather unphysical result and is not in keeping with Flory's original definition of χ. A more conventional χ, which we call χ_f, is

$$\chi_f = (d/L)\chi_S \tag{5}$$

The odd definition of χ used in [SV] does not make any real difference to the results contained in that paper, because one first fixes L and d and then asks what phase has the lowest free energy for these particular values. We thus continue to use χ_S here, but the reader should keep in mind that $\chi_f = \chi_S d/L$ is the physical Flory parameter.

The free energy of the diblock melt is separable into four main terms.

$$F = F_{id} + F_{at} + F_{st} + F_{cs} \tag{6}$$

The first term is an ideal gas entropic term associated with the spatial placement of the chain–rod points of attachment (junction points or joints). In [SV] this was important for some phase transitions, but in the calculations presented here its effect is negligible. The second is the Flory interaction term (eq 4), which, because of the strong incompatibility of the rods and chains, will usually manifest itself here via an interfacial tension γ. F_{st} arises from the steric interactions of the rigid rods with their neighbors. This is modeled in [SV] using a Flory lattice approach. The final term, F_{cs}, is the elastic stretching free energy contributed by the chains. If the chains are strongly stretched, then for one given chain this is

$$F_{cs} = \frac{T}{4a^2}\int_0^N dn \left(\frac{d\mathbf{r}_n}{dn}\right)^2 \tag{7}$$

with $\mathbf{r}_n$ the position of the nth monomer. Here we will be concerned with phases where the chains are essentially grafted onto the chain–rod interface and thus behave like a grafted brush[14-17] with grafting density $\sim 1/d^2$. The height of such a brush is (at least near for lamellar systems) Nv/d^2 which must be much greater than the unperturbed radius of a chain, $\sim N^{1/2}a$, for strong stretching to be valid. This implies we must have $\lambda \gg \nu$, which is easy to achieve, even for $\lambda \ll 1$. Thus the strong stretching approximation is a good one (see also the discussion at the end of section 3). In this paper, it will be F_{at} and F_{cs} that are most important. One might also expect an orientational entropy term in the free energy. This is negligible when comparing free energies of the smectic phases considered here, because all the rods are assumed well-aligned.

We now briefly summarize the phase changes found in [SV] in the limit $\lambda \gg 1$. First, we consider $\kappa \ll 1$, so that the unperturbed radius of the chains is much smaller than the length of the rods. As χ_S is increased from zero there

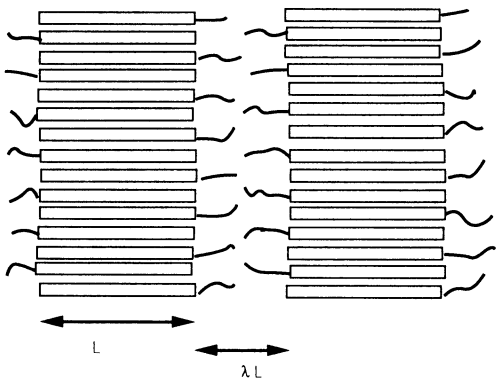

Figure 1. Section of the monolayer lamellar phase discussed in [SV]. The chains only stretch a distance $\lambda L/2$ from the chain–rod boundary, and there is on average $1/(2d^2)$ of chains per unit area.

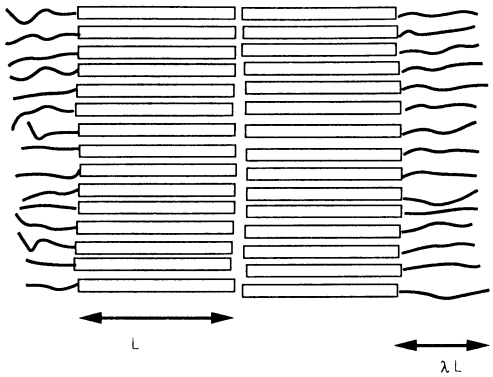

Figure 2. Bilayer lamellar phase. Here the grafting density is $1/(d^2)$ and the chains must stretch a distance λL from the surface to avoid each other.

is a nematic–smectic transition at

$$\chi_S = \chi_{sc} \approx 0.95/\lambda \tag{8}$$

At larger χ_S the system gradually changes so there is a so-called "neutral structure" in which the chains are not strongly stretched. For

$$\chi_S > 0.09\lambda/\kappa \tag{9}$$

a mixed monolayer lamellae system forms, with some chain penetration into the mainly rod monolayers. As χ_S is further increased, the chains are ejected from the rod monolayers until a true complete monolayer phase (Figure 1) is found for

$$\chi_S > \lambda^2/8\kappa \tag{10}$$

In this complete monolayer "phase" the rods form layers into which there are no coils (and vice versa). The transition from the smectic to the complete monolayer phase should be thought of as being gradual so perhaps the term "regime" is more appropriate to describe the completed monolayers. The smectic ordering for χ_S near χ_{Sc} is small, and the flexible chains are slowly ejected from the rod layers until the rod volume fraction in the layers is unity (eq 10). This complete monolayer phase finally changes to a bilayer lamellar phase (Figure 2) for

$$\chi_S > \frac{9}{128}\frac{\lambda^5}{\kappa^3} \tag{11}$$

For $\kappa \gg 1$, so that the chains have large unperturbed radii compared to the rods, the nematic to smectic transition occurs directly to the mixed monolayer state,

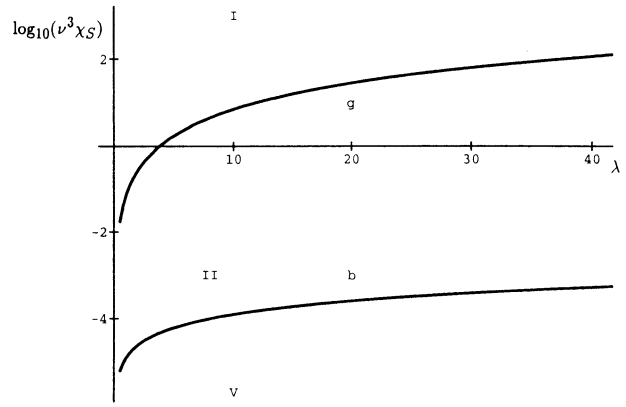

Figure 3. Upper part of the phase diagram from [SV]. log ($\nu^3\chi_S$) is plotted against λ for $\nu = 0.01$. Here I is the bilayer lamellar region, II the monolayer lamellar region, and V the incomplete monolayer region. The curves b and g correspond to eqs 10 and 11, respectively.

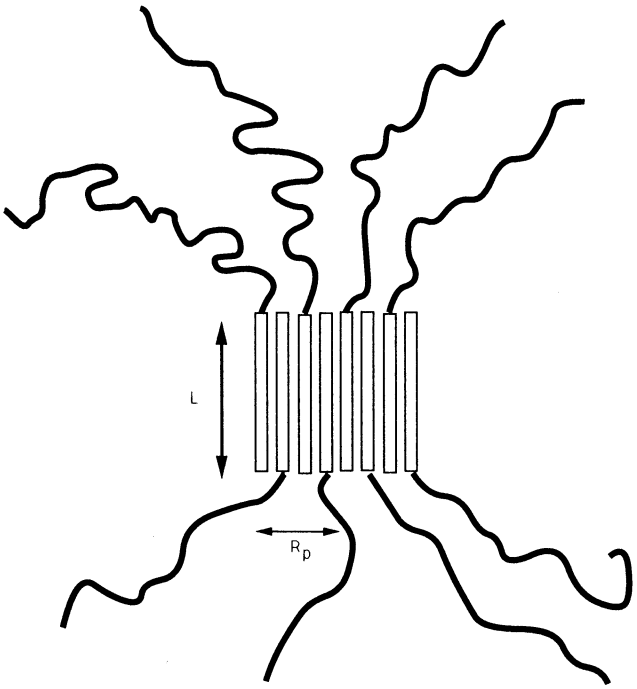

Figure 4. Representation of a monolayer puck. In practice the chains would be much longer and much denser.

at a value of

$$\chi_S = \Gamma\frac{\lambda}{\sqrt{\kappa}} \quad \text{where } \frac{e^{4\Gamma}}{8\Gamma} = \kappa^{1/2} \tag{12}$$

The other transitions then occur as for the $\kappa \ll 1$ case. The part of the phase diagram we shall be interested in is shown in Figure 3.

3. Chain Free Energy for a Puck

In this section we will produce an estimate of the chain-stretching contribution to the free energy of a puck (Figure 4) of radius R_p. For the case of chains grafted to a surface possessing a high degree of symmetry (e.g., a plane, sphere, or cylinder) the calculation of the stretching contribution to the free energy is reasonably straightforward, as it is clear what stretched (classical) trajectories the chains take. In all three cases mentioned there is no bending of the chains and they assume radial trajectories normal to the surface. In [SV] it was assumed for the lamellar case in the limit of strong stretching that not only did the chains point normal to the surface but their ends were all located at a fixed distance from the plane of rod–chain junctions. This in fact is an erroneous assumption, as is known from the self-consistent-field studies of polymer brushes.[14,18] The minimum free energy of a flat brush is achieved by having an end distribution of the form $z/(H^2 - z^2)^{1/2}$ where H is the height of the brush. However, the assumption does give the correct scaling of the stretching energy and merely gives the wrong value ($\simeq$15% overestimate) for a numerical prefactor.

For the case of a hockey puck the calculation of the chain-stretching energy is by no means trivial. In general, one would expect the chains to follow curved trajectories, particularly near the edge of the puck, so as to make use of the volume near the puck sides from which no chains emanate. Close to the upper and lower surfaces of the puck the chains should behave as they would near a planar brush, and far away from the puck the chains can be expected to point radially, as they would for a spherical micelle.

We will first concentrate on the case where $R_p \gg L$ so that the puck is pancakelike. In this case we can treat the upper side of the puck and its lower side separately. The problem then becomes one of a circular region of tethered chains emanating into the upper half plane. This neglects the volume alongside the puck. We assume that the chains want to form a hemispherical shell at a radius of R_s from the disk, as rapidly as they can, with a constant surface density on this shell. After passin through this shell the chains behave as they would for the upper half of a spherical micelle. In order to get from being grafted to the disk to passing through the shell, we assume that they travel in straight line trajectories, consistent with the constant density melt constraint. This calculation has only one free parameter R_s, which we will vary to minimize the free energy. In reality there are an infinite number of free parameters, corresponding to the chain trajectories. Our calculation will thus only provide an upper bound for the free energy, but it will produce the correct scaling with a puck radius.

The coordinates used in the calculation are shown in Figure 5. The number of chains per unit area grafted onto the disk is σ, and we consider a small ring on the disk at radius r and with width dr. The chains starting on this ring travel toward the hemisphere along straight line trajectories via a volume which is approximately a wedge rotated around the z axis. It is assumed that chains from no other ring enter this wedge. By counting the number of chains in the ring and equating it to the number that must pass through the corresponding ring on the hemisphere, one can show that for a uniform surface coverage on the hemisphere

$$r^2 = R_p^2(1 - \cos\theta) \tag{13}$$

Now in order to calculate the stretching term we must determine how the volume allowed to each chain varies with distance from the puck surface. If s is the distance traveled by a chain that makes an angle α with the normal, then

$$dV = 2\pi(r + s\sin\alpha)\left(s + \cos\alpha\frac{dr}{d\alpha}\right) ds\, d\alpha \tag{14}$$

If the nth monomer of a chain which begins at r is located at distance s, then from the incompressibility of the melt

$$2\pi r v\sigma\frac{dn}{ds} dr = \frac{dV}{ds} = 2\pi(r + s\sin\alpha)\left(s + \cos\alpha\frac{dr}{d\alpha}\right) d\alpha \tag{15}$$

If d$Q(r)$ is the number of grafting points within dr of the circle of radius r, then the stretching energy for all the

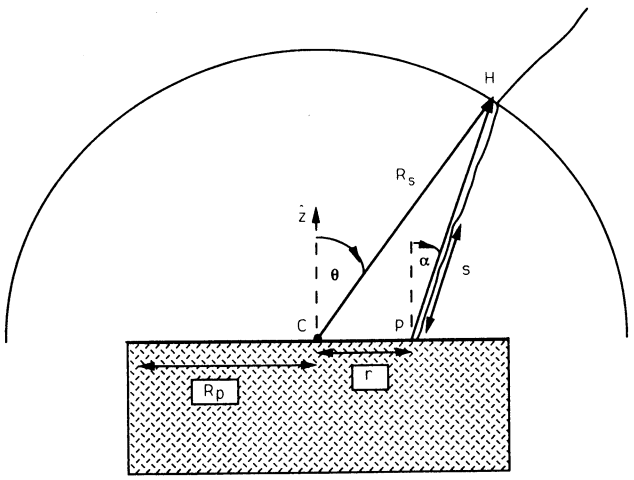

Figure 5. Coordinate system used in the calculation of the chain-stretching free energy for a disk of grafted chains. R_s is the radius of the hemisphere which the chains from the disk approach in such a manner that they produce a uniform grafting density over it. After the chains have passed this hemisphere they are assumed to have radial trajectories, as if they emanated from the center point C. Here a chain starts from the ring at radius r (measured in the plane of the puck) (point P) and makes its way, via a straight path, to the hemisphere (point H). α measures the angle the chain trajectory makes with the normal to the puck and is constant for a chain starting from a given radius. θ is the angle the line from the chain's point of intersection with the hemisphere to the puck center (line CH) makes with the puck normal. s is the arc length of the given chain, measured from the point P.

chains out to the hemispherical shell is

$$F_h = \frac{1}{4a^2}\int_0^{R_p}\frac{dQ}{dr}\,dr\int_0^{s_m(r)}ds\,\frac{ds}{dn} = \frac{2\pi\sigma^2\upsilon}{4a^2}\int_0^{R_p}dr\,\frac{r^2}{r\frac{d\alpha}{dr}-\cos\alpha\sin\alpha}\times \log\left[\frac{r(\cos\alpha + s_m\,d\alpha/dr)}{r\cos\alpha + s_m\sin\alpha\cos\alpha}\right] \quad (16)$$

Here the angle the chains make with the normal α is related to the radial starting point of the chains via

$$\tan\alpha = \frac{(2r^2R_p^2 - r^4)^{1/2} - rR_p^2R_s^{-1}}{R_p^2 - r^2} \quad (17)$$

and the maximum s for each ring of chains is given by

$$s_m(r) = \left[R_s^2 + r^2 - 2rR_s\left[\frac{2r^2}{R_p^2} - \frac{r^4}{R_p^4}\right]^{1/2}\right]^{1/2} \quad (18)$$

The remaining term in the free energy is the contribution from the chain portions outside the hemisphere. This is approximately

$$F_o \simeq \frac{\pi}{2}\frac{\upsilon\sigma^2}{4a^2}R_p^4\left(\frac{1}{R_s} - \left(\frac{2}{3R_p^2\sigma Ld^2\lambda}\right)^{1/3}\right) \quad (19)$$

The second term here is due to the finite length of the chains. In calculating it we have assumed that the monomers outside the hemisphere are equally distributed between all the chains. In practice this is not exact, because some of the chains, particularly those near the disk center, have used up more of their monomers in getting to the hemisphere. The whole expression in eq 19 must not be negative. It becomes negative when the radius of the hemisphere is so large that there is not enough polymer to fill it. Upon adding this to eq 16 and defining $\rho = R_s/R_p$, one finds the total stretching free energy is

$$F_s = \frac{\pi\sigma^2\upsilon R_p^3}{2a^2}\left[f(\rho) + \frac{1}{4\rho} - \frac{1}{4}\left(\frac{2R_p/L}{3\sigma d^2\lambda}\right)^{1/3}\right] \quad (20)$$

where $f(\rho)$ is a dimensionless integral (obtained from eq 16), which increases monotonically with ρ for the case we are interested in. Two conditions must be obeyed by ρ in eq 20 for this expression to be valid. The first is $\rho > 1$ which ensures that the hemisphere covers the entire puck, and the second is

$$\rho < \rho_c \equiv (3\sigma Ld^2\lambda/2R_p)^{1/3} \quad (21)$$

which makes eq 19 positive. When eq 20 is minimized with respect to ρ, the resulting free energy is

$$F_s = \frac{\pi\sigma^2\upsilon R_p^3}{2a^2}\left[\beta - \frac{1}{4}\rho_c^{-1/3}\right], \quad \rho_c > 1.28 \quad (22)$$

where $\beta \approx 0.4376$ and the extremum ratio of the sphere radius to the disk radius is $\rho \approx 1.28$. For the case of short chains so that $1 < \rho_c < 1.28$ the free energy will be given by a hemisphere which just encloses all the polymers, so that

$$F_s = \frac{\pi\sigma^2\upsilon R_p^3}{2a^2}f(\rho_c) \approx 0.2\frac{\pi\sigma^2\upsilon R_p^3}{2a^2}, \quad 1 < \rho_c < 1.28 \quad (23)$$

For $\rho_c < 1$ it is impossible to form any hemisphere and the disk will behave like a planar brush, as the chains are not long enough to explore the volume available away from the plane. Thus

$$F_s \approx \frac{\pi\sigma^2\upsilon R_p^3}{2a^2}\frac{\rho_c^3}{3}, \quad \rho_c < 1 \quad (24)$$

Therefore, for small puck radii R_p such that $\rho_c \gg 1$ the puck has a "mop" and the free energy scales as R_p^3 (eq 22), whereas at large puck radii, such that $\rho_c \ll 1$, the puck is essentially "crew cut" and the free energy scales as R_p^2 (eq 24). One way of interpreting this is to say at large R_p the chains behave as a planar brush whose height is fixed by the chain dimensions, so the stretching free energy = $\mathcal{F}\pi R_p^2$, where $\mathcal{F}$ is the free energy per unit area. In contrast, at small R_p the chains initially see a flat surface, but once they have traveled a distance R_p they can explore a spherical shell. Hence, there is an extra factor of R_p, which is essentially the height of the brush. In this paper we will mainly be concerned with mops. By behaving as planar brushes, crew-cut pucks lose the chain-stretching advantage, which is the main reason for studying them.

In deriving the free energy expressions above we assumed that $R_p \gg L$ so that the chains emerging from each side of the puck were restricted to a hemisphere. For a very thin puck $R_p \ll L$, in the limit of long chains, each side of the puck will have its own sphere, with a small volume removed from it caused by the presence of rods. This will allow a further decrease in energy over the hemispherical case, because the chains can explore a larger volume and hence stretch less. This will not change the form of eq 22, but it will provide a slightly different prefactor. Hence, there is in effect a weak function of L multiplying (eq 22), which we have ignored here.

One more point about our chain-stretching energy needs to be made. We have assumed that strong chain stretching is always valid (eq 7). For lamellar systems one can argue that if it is valid near the grafting surface, then it is valid everywhere because the amount of volume per unit contour length that becomes available to the chains is a constant (at least in the mean-field case—this is not entirely true

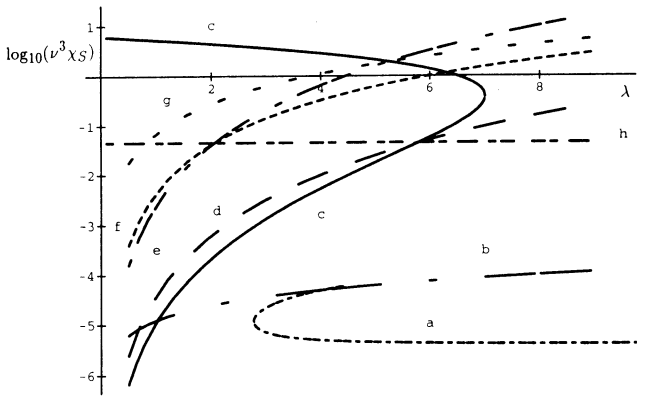

Figure 6. Graph of the curves bounding the various regions discussed in section 4. log ($\chi_S\nu^3$) is plotted against λ. Curves a–h are eqs 44, 10, 42, 31, 40, 43, 11, and 45, respectively.

in the more correct self-consistent calculations[14,18]) as the chain moves away from the surface. However, for chains grafted onto a sphere (which is approximately the case here) at large distances this is not true—the chains have to stretch less and less as they move away from the grafting surface. Of course, it is just this effect that makes nonlamellar phases energetically attractive. One can get a rough idea of when the strong stretching approximation will break down by considering a sphere grafted with Q chains. We then equate dr/dn to the characteristic "stretching" of a Gaussian chain $\sim 2a$ and obtain a radius $r = Qv/a^2$ at which strong stretching breaks down. For the puck case this corresponds to a distance from the puck surface of $r \sim R_p^2/(\nu L)$. It is shown later (section 4) that pucks first occur with radii of $R_p \sim L(\nu^3\chi_S)^{1/4}$, yielding a distance $r \sim R_p\chi_S^{1/4}\nu^{-1/4}$ at which chain stretching breaks down. Now $\nu \ll 1$ and in general $\chi_S \gg \nu$ so that this radius is very large (i.e., much larger than the effective hemisphere). At such large radii the energy contributed to the puck by the chains in the strong stretching approximation is negligible and so its inclusion here does not alter our arguments. Of course, if strong stretching were to break down at a small distance from the puck surface, then it would lead to puck phases being even more favorable compared to lamellar phases, as this is not an effect which occurs significantly in the latter.

4. Comparison of the Puck with Lamellar Phases

Having calculated the stretching free energy of a puck, we are now in a position to compare the puck to the lamellar phases. One way to do this is to break up a given area A of the lamellar phase. This is equivalent to comparing the free energies per chain. We will first break up a monolayer into monolayer pucks of radius R_m. The puck phase differs from the monolayer phase in only two ways that are relevant to the free energy. The puck phase has a different stretching free energy, and it has an extra curved surface that gives it more surface energy. There is also a translational entropy difference which proves negligible. To compute the surface energy component, we use the surface tension calculated in [SV] of

$$\gamma = \frac{1}{d^2\sqrt{2}}(\nu\chi_S)^{1/2} \tag{25}$$

There are $A/(\pi R_m^2)$ pucks, each with an extra curved surface of $2\pi R_m L$, and so the extra surface free energy is just

$$F_\gamma = 2\gamma A/x \tag{26}$$

where we have defined $x = R_m/L$. For the stretching energy

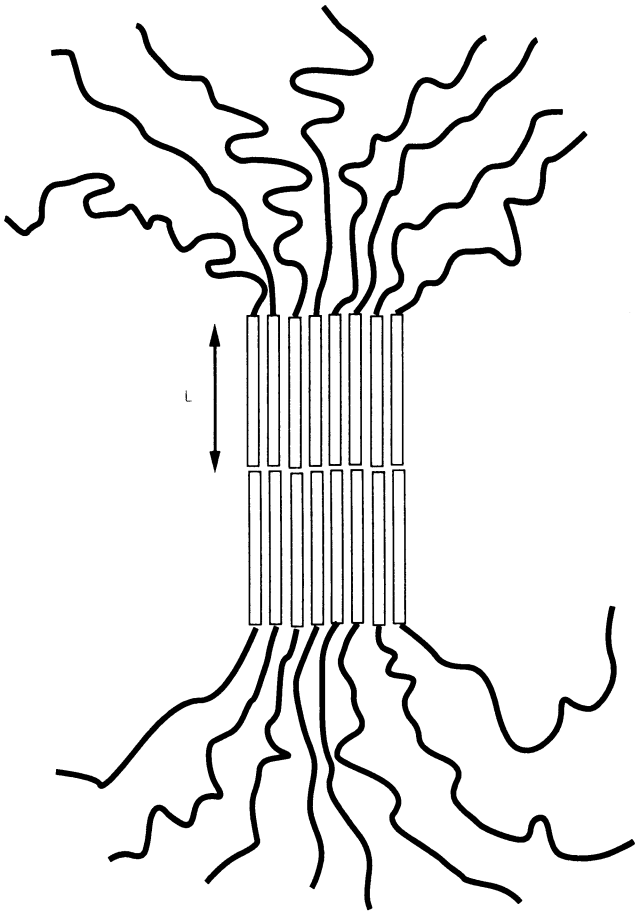

Figure 7. Representation of a bilayer puck.

of each puck we will use eq 22 (we shall verify the validity of this later). Noting that $\sigma = 1/(2d^2)$ and that each puck has two sides, the stretching term (for *all* the disks) is

$$F_{ms} = \frac{A\lambda x}{4\kappa d^2}\left(\beta - \frac{1}{4}\left(\frac{4x}{3\lambda}\right)^{1/3}\right) \tag{27}$$

This is to be contrasted with the stretching term from the monolayer lamellae, which is

$$F_{ls} = \frac{A\lambda^2}{16d^2\kappa} \tag{28}$$

The difference between the free energies is then

$$\Delta F = F_\gamma + F_{ms} - F_{ls} \propto \frac{\sqrt{2}(\nu\chi_S)^{1/2}}{x} + \frac{\lambda x}{4\kappa}\left(\beta - \frac{1}{4}\left(\frac{4x}{3\lambda}\right)^{1/3}\right) - \frac{\lambda^2}{16\kappa} \tag{29}$$

As a first approximation we can neglect the $x^{1/3}$ correction to the puck stretching (verified below), which on minimization yields

$$x = (4/\beta)^{1/2}(2\nu^3\chi_S)^{1/4} \tag{30}$$

Substitution into eq 29 leads to the following condition on χ_S for the free energy to be negative, and hence monolayer pucks favored

$$\chi_S < 3.98 \times 10^{-5}\lambda^4/\nu^3 \tag{31}$$

From [SV] we know that monolayer lamellae form in the region

$$0.125\lambda\nu^{-1} < \chi_S < 0.07\lambda^2\nu^{-3} \tag{32}$$

Thus the monolayer lamellae will be of higher free energy than the monolayer pucks in the following region of the

phase diagram:

$$0.125\lambda\nu^{-1} < \chi_S < \begin{cases} 3.98 \times 10^{-5}\lambda^4/\nu^3, & \text{if } \lambda < 41.92 \\ 0.07\,\lambda^2\nu^{-3}, & \text{if } \lambda > 41.92 \end{cases} \quad (33)$$

For $\lambda > 42$ pucks dominate the region formerly thought to consist of monolayer lamellae. The phase boundaries delineated by eqs 31 and 32 can be seen in Figure 6.

We now justify the use of eq 22 in eq 29. What is required is that the $(x/\lambda)^{1/3}$ correction term be small and, what amounts to much the same thing, $\rho < \rho_c$. Using the solution in eq 30 for x, we find the condition

$$\chi_S < 0.04\lambda^4/\nu^3 \quad (34)$$

must be obeyed. From eq 31 we can see that in the region of interest this is the case.

There are four main phases whose energies we need to compare in order to amend the phase diagram. Apart from the monolayer puck phase considered above, one can also imagine other puck phases, in particular, a bilayer puck (Figure 7), which consists of bilayer lamellae cut into pieces. The free energy of this system may be calculated in a similar way, noting that $\sigma = 1/d^2$. The free energies (per polymer molecule) of the four phases are

$$F_{ml} = \frac{\lambda}{16\nu} + \frac{2}{\nu}\left(\frac{\nu^3\chi_S}{2}\right)^{1/2} \quad (35)$$

$$F_{mp} = \frac{\sqrt{\beta}}{\nu}(2\nu^3\chi_S)^{1/4} + \frac{2}{\nu}\left(\frac{\nu^3\chi_S}{2}\right)^{1/2} \quad (36)$$

$$F_{bp} = \frac{\sqrt{2}\sqrt{\beta}}{\nu}(2\nu^3\chi_S)^{1/4} + \frac{1}{\nu}\left(\frac{\nu^3\chi_S}{2}\right)^{1/2} \quad (37)$$

$$F_{bl} = \frac{\lambda}{4\nu} + \frac{1}{\nu}\left(\frac{\nu^3\chi_S}{2}\right)^{1/2} \quad (38)$$

Here m, b, l, and p refer to monolayer, bilayer, lamellae, and puck, respectively. In deriving the puck energies, we have already minimized the free energy over the puck radius. For the monolayer puck, the result x_m is that given by eq 30, whereas for the bilayer pucks $x_b = x_m/\sqrt{2}$. Thus bilayer systems form smaller pucks than monolayer systems, but for a given number of polymer molecules in the system their number is the same in both cases. The second term in each of the free energies is contributed by the flat surfaces at the chain–rod interface. The area of these surfaces is of course half as much in the bilayer puck case.

We can now compare a monolayer puck phase with a bilayer puck phase. One finds that the bilayer pucks dominate for

$$\chi_S > 0.045/\nu^3 \quad (39)$$

and that, at the point of crossover between monolayers and bilayers, $x_m = 1.66$. The reason why bilayer pucks dominate monolayer pucks at large χ_S is the same as for the lamellae case; i.e., at large values of the Flory parameter it is the chain–rod surface terms which dominate the extra stretching energy which a bilayer system has. Comparison between the bilayer puck phase and the bilayer lamellae phase shows that the bilayer pucks dominate for

$$\chi_S < 0.00255\lambda^4\nu^{-3} \quad (40)$$

The competition between bilayer pucks and monolayer lamellae yields

$$\Delta F = F_{bp} - F_{ml} \propto \sqrt{2}\sqrt{\beta}(2\nu^3\chi_S)^{1/4} - \left(\frac{\nu^3\chi_S}{2}\right)^{1/2} - \frac{\lambda}{16} \quad (41)$$

The monolayer lamellae is the more stable of the two phases for

$$\frac{2}{\nu^3}(\sqrt{\beta} - (\beta - \lambda/16)^{1/2})^4 < \chi_S < \frac{2}{\nu^3}(\sqrt{\beta} + (\beta - \lambda/16)^{1/2})^4 \quad (42)$$

This puts a "nose" on the phase diagram. At low χ_S the bilayer puck is more stable because it contributes less chain-stretching free energy. As χ_S is increased, the extra curved surface of the puck phase makes it unstable. However, on further increasing χ_S the extra flat surface area of the monolayer phase means it is no longer favored. The final comparison between true monolayer phases is for monolayer pucks and bilayer lamellae. The region in which the monolayer pucks dominate is

$$\chi_S < \frac{1}{2\nu^3}(-\sqrt{\beta} + (\beta + \lambda/2)^{1/2})^4 \quad (43)$$

There is at least one other phase worth considering here. This is the incomplete monolayer phase discussed in [SV]. In this phase the monolayers of rods are not packed densely, so that some chains are allowed to interpenetrate the rod monolayers. The free energy of this phase was calculated in [SV] and is reproduced using the present notation in the appendix. Formerly this phase bounded the monolayer lamellae phase below $\lambda/(8\nu)$. It is now bounded by the monolayer puck phase. The locus of the transition between the two is found by comparing eq 36 with the free energy given in the appendix and is

$$\lambda = \frac{\nu^{1/4}\chi_S\sqrt{2}\left(\frac{3}{2} - \frac{3}{64\chi_S\nu} + 4\chi_S\nu\right)}{\nu^{1/4}\chi_S\sqrt{2} - 2^{3/4}(\beta)^{1/2}\chi_S^{1/4} - 2(\chi_S)^{1/2}\nu^{3/4}} \quad (44)$$

As can be seen from Figure 6 this produces another nose in the phase diagram, although it may be spurious, as it occurs at such a small value of λ. For large λ the boundary line separating the two regions becomes straight, and the monolayer pucks dominate the incomplete phase for

$$\chi_S > \beta^{2/3}(\nu/2)^{-1/3} \quad (45)$$

In comparing the two phases, an approximation is made. The free energy of the incomplete phase was calculated assuming only a bulk Flory term and no contribution from the walls. The puck calculation used exactly the opposite assumptions. In the boundary region between the two phases these expressions will only be approximately correct, so the boundary line (eq 44) only gives an approximate indication of where the transition is likely to take place. In reality one expects to find incomplete hockey puck phases—that is, phases where the chains penetrate the pucks. In such a regime, because the pucks no longer pay a significant surface penalty but still gain a stretching advantage, one expects the incomplete pucks to dominate over incomplete lamellar phases. Of course, both types of geometry pay the same bulk mixing penalty.

By using all the inequalities derived in this section with the help of Figure 6, one can schematically construct the

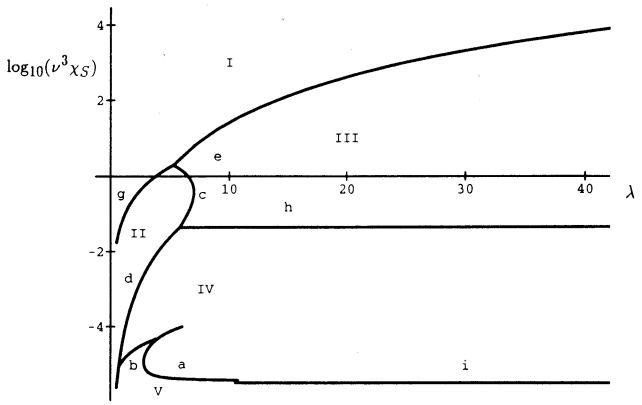

Figure 8. Phase diagram including the hockey puck phases. Again we plot log ($\nu^3\chi_S$) against λ. The phases are (I) bilayer lamellae, (II) monolayer lamellae, (III) bilayer hockey pucks, (IV) monolayer hockey pucks, and (V) incomplete monolayer lamellae. The curves are the same as those in Figure 6, with curve i being eq 39. If radially packed micelles or incomplete hockey pucks exist, they should be found in the vicinity of curve i. The reader should note that regions II and V should probably not be considered as distinct phases—there is a gradual change between the two as flexible chains are expelled from the monolayers.

phase diagram for the system, which is shown in Figure 8.

5. Spherical and Radially Packed Cylindrical Micelles

Having considered the case of hockey puck micelles, we now turn our attention to spherical and cylindrical micelles. An immediate difficulty arises here if one tries to pack the rods into such shapes. For small-molecule nematic liquid crystals it is possible to pack the molecules into a sphere both radially and axially.[19] In the case considered here, the attachment of long rods to incompatible coils implies that for a spherical system only the radial packing offers any energetic advantages. An important question to ask is, can rods of length L be packed radially into a sphere of radius R so that they completely fill the space within the sphere? The answer is yes, that the volume fraction of rods can be made unity in a certain region but that there will always be a significant fraction of the rods sticking out the ends. To show this, we use a lattice model and take the continuum limit. We divide space into spherical shells of thickness l and divide the jth shell at radius jl into n_j cells of volume ld^2, so that

$$n_j = 4\pi j^2 (l/d)^2 \tag{46}$$

If we start N_k rods in layer k, then the number of available sites for starting rods in layer i is

$$\tilde{n}_i = 4\pi i^2 (l/d)^2 - \sum_{j=\max(1,i-L/l)}^{i-1} N_j \tag{47}$$

We now take the continuum limit of this and say $i = r/l$, $N_j = lN(jl)$ (so that $N(r)\,dr$ is the number of rods that begin in a shell between r and $r + dr$) and

$$\sum_{j=\min(1,i-L/l)}^{i-1} N_j = \frac{1}{l}\int_{\max(0,r-L)}^{r} dr\, lN(r) \tag{48}$$

so that if all the sites in each shell are filled, then

$$lN(r) = 4\pi(r/d)^2 - \int_{\max(0,r-L)}^{r} dr\, N(r) \tag{49}$$

We now need to impose a lower cutoff on l. This we take to be d. For $l < d$ the continuum approximation breaks down. We can then say (for the case of interest where $r < L$)

$$\frac{dN(r)}{dr} = \frac{8\pi r}{d^3} - \frac{N(r)}{d} \tag{50}$$

which has the solution

$$N(r) = \frac{8\pi}{d}\left(\frac{r}{d} - 1 + \exp(-r/d)\right) \tag{51}$$

The boundary conditions being $N(0) = 0$, i.e., there are not ends inside the sphere of zero radius. This is thus the profile for rod ends which packs the sphere to unit density. We note that the exponential term decays rapidly, so that the number of chain ends per unit volume is given by (for $r \gg d$, $r < L$)

$$\rho(r) = 2/d^2 r \tag{52}$$

The density of new rods goes down as $1/r$, although their actual number goes up as r. Thus, if we stop packing the sphere suddenly at a particular radius, we can expect it to look very spiky. It will not have a clean edge. This in turn implies a large Flory term in the free energy.

To examine this more closely, we take a particular example of packing. The rods are packed with the profile given by eq 52 out to a radius $R < L$, and then no new rods are put in. The volume fraction occupied by the rods may be shown to have the profile

$$\phi_r(r) = \begin{cases} 1, & r < R \\ (R/r)^2, & R < r < L \\ (R^2 - L^2)/r^2 + 2L/r - 1, & L < r < R + L \\ 0, & R + L < r \end{cases} \tag{53}$$

The decay length outside of the ball is initially R, and the volume fraction decay is inverse squared. Thus for a maximally packed ball of radius $R < L$, one can expect a region on the order of the volume of the ball in which there are a significant number of rod monomers. Similar calculations can be performed for a radially packed cylinder of length r where $N(r) = 2\pi L/d$ so that the surface mixing of rods and chains will again be large. It is possible to increase the sharpness of the rod–chain surface slightly by reversing the direction of some of the rods. This would create a shell of rods trapped between two volumes of chains. While there may exist a small region of the phase diagram where radially packed micelles exist, it is probably at such a low value of χ_S that it is experimentally unattainable, and so we do not consider such micelles here.

6. Discussion and Conclusion

On comparing the two phase diagrams (Figures 3 and 8), one sees how important hockey pucks are likely to be in rod–coil diblocks. The region formerly thought to consist of a monolayer lamellar phase has been reduced in size and is now limited to a region where $\lambda < 7$. It has been replaced mainly by a bilayer puck phase but also in part by monolayer pucks (the region between d and b in Figure 6). The bilayer lamellae region has also been reduced. Of course, for large enough χ_S bilayer lamellae eventually dominate because they have less rod–coil interfacial surface per molecule than any other geometrical configuration. Monolayer hockey pucks now occupy some of the region formerly composed of the incomplete monolayer phase of [SV]. Our calculations have involved putting an upper bound on the stretching energy of the chains, and thus the regions occupied by pucks are probably larger than those calculated here.

There are several other possible phases for which we have provided no detailed calculations but which may exist,

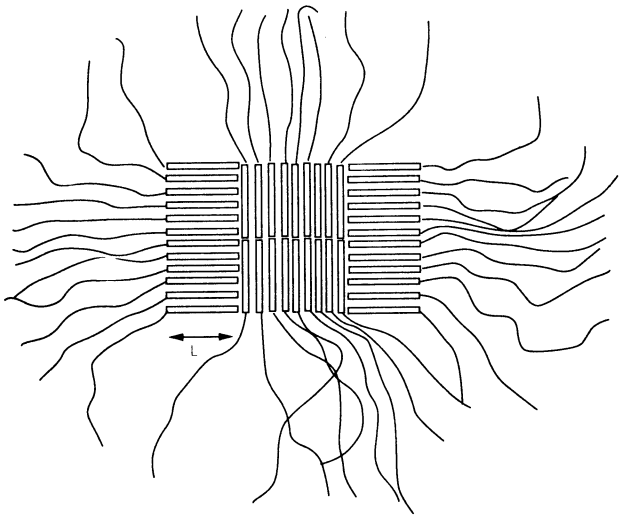

Figure 9. Cross section of an alternative to a hockey puck. This is an attempt to make the entire outer surface rod ends, without forming a sphere.

particularly at low χ_S and large λ. These phases include incomplete hockey pucks, with some chains penetrating the pucks, and possibly radially packed micelles. The latter are particularly volatile because their rod packing always leaves large gaps in the micelle which must be filled with incompatible chains. It is not difficult to show that such "incomplete" phases probably do not exist. From eq 45 we have an approximate condition for the incomplete monolayer phase to be present, $\chi_S^3 < L/l$, where l is roughly the persistence length of the flexible chains. However, we also know from eq 5 that $\chi_S = L\chi_f/d$ where χ_f is the Flory χ parameter. We then get

$$\chi_f < \frac{d}{l}\left(\frac{d}{L}\right)^2 \ll 1 \tag{54}$$

an unlikely condition for incompatible rod–coil copolymers.

One may also imagine other kinds of tightly packed micelles like that shown in Figure 9. These micelles represent an attempt to form spheres without the associated packing problems. For certain regions of the phase diagram (λ large and χ_S near the bilayer puck region) these micelles might have a free energy advantage over pucks, for they project less interfacial area per rod. However, they also crowd more grafted flexible chains into a small region and thus pay a larger stretching penalty. Their comparison with pucks would require a more exact model of chain stretching than is presented in this paper.

Here we have only considered isolated noninteracting micelles. In practice the micelles will interact and will pack to form ordered phases. However, their interaction will depend strongly on how each perturbs the surrounding chains of the other. Thus a calculation of the micelle–micelle interaction, which will vary not only with distance but with direction (for pucks), would require a detailed knowledge of the spatial chain distribution. Even for the case of the isolated pucks considered here this is not readily available.

Acknowledgment. We acknowledge useful discussions with Phil Pincus and Alexei Khokhlov. D.R.M.W. was supported by DOE Grant DE-G03-87ER45288. G.H.F. is grateful to the National Science Foundation for support under PYI Grant DMR-9057147.

Appendix: The Incomplete Monolayer Regime

In [SV] a regime that exists for $\lambda \gg 1$ and for small χ_S was described. This consists of incomplete monolayer lamellae of thickness L, consisting of a mixture of rods and some chains, with the intervening layer of thickness SL consisting entirely of chains. The volume fraction of rods in the monolayers is $\eta_{max} \approx (1 + S)/\lambda$. This phase is dominant at low enough χ_S because it enables the chains to stretch less. The penalty paid is a bulk Flory term, which ultimately destroys the phase at high χ_S. Here we convert the free energy given in [SV] into a free energy per polymer molecule in our units and with our zero of energy. Our starting point is 5.6 of [SV]. There the "free energy per unit length" is

$$\mathcal{F} = -\frac{\chi_S}{\lambda^2}(1 + S) + \frac{1 - S + S^2}{16\kappa\lambda} \tag{55}$$

which means that the free energy of a section of lamellae of area A and height Δz is, in dimensional units

$$F'_s = -\frac{A\delta z}{d^2 L}\left\{\frac{\chi_S}{\lambda^2}(1 + S) + \frac{1 - S + S^2}{16\kappa\lambda}\right\} \tag{56}$$

We require the free energy per polymer molecule. To get this, we have $\Delta z = (1 + S)L$ and $A = d^2/\eta_{max}$, yielding

$$-\frac{\chi_S}{\lambda}(1 + S) + \frac{1 - S + S^2}{16\kappa} \tag{57}$$

This expression still differs from the one required because when the monolayer becomes complete (i.e., all the chains have been expelled from it), $(1 + S)/\lambda = 1$ and the bulk Flory term, which we would like to be zero in such a case, is $-\chi_S$. Thus the free energy per rod is in fact

$$F_S(S) = \chi_S - \frac{\chi_S}{\lambda}(1 + S) + \frac{1 - S + S^2}{16\lambda\nu} \tag{58}$$

which upon minimization with respect to S yields

$$F_S = \chi_S - \frac{\chi_S}{\lambda}\left(\frac{3}{2} + 4\nu\chi_S - \frac{3}{64}\frac{1}{\chi_S\nu}\right) \tag{59}$$

References and Notes

(1) Semenov, A. N.; Vasilenko, S. V. *Sov. Phys. JETP* **1986**, *63*, 70.
(2) Leibler, L. *Macromolecules* **1980**, *13*, 1602.
(3) Semenov, A. N. *Sov. Phys. JETP* **1987**, *66*, 712.
(4) Helfand, E.; Wasserman, Z. In *Developments in Block Copolymers*; Goodman, I., Ed.; Applied Science: New York, 1982.
(5) Bates, F. S.; Fredrickson, G. H. *Annu. Rev. Phys. Chem.* **1990**, *41*, 525.
(6) Halperin, A. *Macromolecules* **1990**, *23*, 2724.
(7) Vilgis, T.; Halperin, A. *Macromolecules* **1991**, *24*, 2090.
(8) Whitmore, M. D.; Noolandi, J. *Macromolecules* **1988**, *21*, 1482.
(9) Ronca, G.; Yoon, D. Y. *J. Chem. Phys.* **1985**, *83*, 373.
(10) Yoon, D. Y.; Bruckner, S. *Macromolecules* **1985**, *18*, 651.
(11) Flory, P. J. F.; Matheson, J. *J. Phys. Chem.* **1984**, *88*, 6606.
(12) Grosberg, A. Y.; Khokhlov, A. R. *Adv. Polym. Sci.* **1981**, *41*, 53.
(13) Fredrickson, G. H.; Leibler, L. *Macromolecules* **1990**, *23*, 531.
(14) Milner, S. T.; Witten, T. A.; Cates, T. T. *Macromolecules* **1989**, *22*, 853.
(15) Alexander, S. *J. Phys. Fr.* **1977**, *38*, 983.
(16) de Gennes, P.-G. *J. Phys. Fr.* **1976**, *37*, 1443.
(17) de Gennes, P.-G. *Macromolecules* **1980**, *13*, 1069.
(18) Semenov, A. N. *Sov. Phys. JETP* **1985**, *62*, 733.
(19) Erdmann, J. H.; Žumer, S.; Doane, J. W. *Phys. Rev. Lett.* **1990**, *64*, 1907.